Hepatology Research 2008; **38**: 800–809 doi: 10.1111/j.1872-034X.2008.00339.x

Original Article

Effect of selective cyclooxygenase-2 inhibitor meloxicam on liver fibrosis in rats with ligated common bile ducts

Seong Min Kim,[1] Ki Chung Park,[1] Ho Guen Kim[2] and Seok Joo Han[1]

Departments of [1]Surgery and [2]Pathology, Yonsei University College of Medicine, Seoul, Korea

Aim: Cholestasis triggers fibrogenesis in the liver. Hepatic cyclooxygenase-2 (COX-2) expression increases in various chronic liver diseases caused either by viruses or toxins. We hypothesized that selective COX-2 inhibitor meloxicam could suppress inflammation and fibrogenesis in a rat model of cholestasis induced by bile duct ligation (BDL).

Methods: Forty-three Sprague–Dawley rats were assigned to one of four treatment groups (sham-operation, BDL, daily meloxicam injections following BDL, and daily meloxicam injection without BDL). Liver histopathology was analyzed with hematoxylin–eosin and Masson's trichrome staining. The expression of α-smooth muscle actin (α-SMA), transforming growth factor-β1 (TGF-β1), and COX-2 were measured with immunohistochemical staining. The levels of COX-2, TGF-β1, and matrix metalloproteinase-9 (MMP-9) production were measured with the Western blot method and an enzyme immunoassay.

Results: Meloxicam treatment attenuated the expression of α-SMA, TGF-β1, and COX-2 in rats that were treated with BDL for 3 weeks. This was associated with a marked reduction in collagen accumulation and histological improvement. In addition, meloxicam treatment was found to downregulate the levels of hepatic COX-2, TGF-β1, and MMP-9 production.

Conclusion: Cholestasis in BDL rats induces hepatic COX-2 expression. Selective COX-2 inhibitor meloxicam reduces BDL-induced hepatic fibrosis, and this is associated with reduced hepatic TGF-β1 expression as well as decreased cyclooxygenase activity in the liver.

Key words: α-smooth muscle actin, bile duct ligation, biliary fibrosis, hepatic stellate cells, selective cyclooxygenase-2 inhibitor, transforming growth factor-β1

INTRODUCTION

LIVER FIBROSIS IS a consequence of the wound healing process for chronic liver injury. One of the important mechanisms of liver fibrosis is cholestasis. In chronic cholestasis, inflammation stimulates hepatic myofibroblasts to produce collagen. The upregulation of cyclooxygenase (COX)-2 has been demonstrated in human liver cirrhosis as a result of active inflammation.[1,2] The highest COX-2 expression levels are found in patients with liver cirrhosis. In fact, COX-2 expression levels are higher in patients with liver cirrhosis than those with hepatocellular carcinoma.[3] COX has two isoforms: COX-1 and COX-2. Unlike COX-1, which has a constitutional expression and plays a physiological function, COX-2 is highly induced by inflammation, mitogenic stimuli, and various growth factors. Induction of the COX-2 enzyme results in prostaglandin synthesis in inflamed tissues and neoplastic cells.[4] This is related to the fact that COX-2 is a regulatory enzyme that is involved in the synthesis of prostaglandin and their metabolites in inflammation, cellular proliferation, anti-apoptosis, cell growth, and angiogenesis. Therefore, COX-2 inhibition is an attractive pharmacological target for reducing prostaglandin production at the sites of chronic inflammation and fibrosis. The antifibrotic effect of COX-2 inhibitors was previously reported in several *in vivo* and *in vitro* experiments, such as renal interstitial fibrosis[5] and desmoplasia in several cancers, such as colon,[6] stomach,[7] and breast.[8] There is already good evidence that selective COX-2 inhibitors play a role as antifibrotic agents in the liver.[3,9–11] However, there have been no studies on the effect of selective COX-2 inhibitors on fibrosis in the liver induced by biliary obstruction. We hypothesized that

Correspondence: Dr Seok Joo Han, Division of Pediatric Surgery, Department of Surgery, Yonsei University College of Medicine. #134 Shinchon-dong, Seodaemun-gu, Seoul 120-752, Korea. Email: sjhan@yuhs.ac

Received 27 May 2007; revision 13 December 2007; accepted 16 January 2008.

the suppression of COX-2 has the potential to suppress liver fibrosis induced by biliary obstruction. We designed an animal model of cholestatic liver by common bile duct ligation (BDL), an established animal model of cholestatic liver disease in humans.[12] We used this model to evaluate the effect of COX-2 inhibition on liver fibrogenesis.

METHODS

Animals and experimental designs

FORTY-THREE SPRAGUE–DAWLEY rats (male, 250–300 g) were used in our experiments. The animals were housed in cages for 7 days. The experiments were approved by the Animal Experiment Committee of Yonsei University (Seoul, Korea). The rats were anesthetized with an intramuscular injection of Zoletil (Virbac, Carros, France). The animals were assigned to one of four treatment groups: the sham-operation group (group A, $n = 5$), the BDL group (group B, $n = 17$), the BDL + meloxicam group (group C, $n = 16$), and the meloxicam group (group D, $n = 5$). For group C rats, meloxicam (Mobic, Boehringer Ingelheim, Seoul, Korea) was injected intramuscularly at 1.6 mg/kg/day beginning 48 h after the BDL.[13,14] For group D rats, meloxicam was injected daily without BDL. During the 3 weeks of experimental treatment, the animals were housed in cages equipped with tap water and rat chow under 12/12 h dark/light cycle conditions.

Tissue preparation

After 3 weeks, the animals were given an intraperitoneal injection of sodium pentobarbital (50 mg/kg) and then killed by cardiac puncture. Blood samples were also obtained. A liver biopsy was taken and fixed in 10% buffered formalin solution. The remaining liver tissue was removed en bloc, frozen in liquid nitrogen, and stored at −80°C.

Serum biochemistry

For testing the liver function in rats with hepatic fibrosis, the activities of aspartate transaminase (AST), alanine transaminase (ALT), and the contents of total bilirubin (Tbil) in the serum were determined after 3 weeks of experimental treatment using an automated analyzer (RA-XT, Technicon, Tarrytown, NY, USA).

Hematoxylin–eosin and Masson trichrome staining, and quantification of liver fibrosis by computerized morphometry

Formalin-fixed, paraffin-embedded liver biopsy specimens (5-μm sections) were processed routinely for hematoxylin–eosin staining (HE). For Masson's trichrome staining, tissues were deparaffinized and rehydrated through a graded alcohol series. Slides were incubated sequentially at room temperature (RT) in Weigert's iron hematoxylin, Biebrich scarlet-acid fuchsin, and phosphomolybdic–phosphotungstic acid for 10 min each until the collagen was not red. The sections were transferred directly (without rinsing) to aniline blue solution and stained for 5 min. The slides were washed once with distilled water, and in order to dehydrate the tissue, the slides were incubated in a graded alcohol series ending with xylene. Finally, coverslips were fixed with Permount (Fisher Scientific, Fair Lawn, NJ, USA). The degree of fibrosis was measured using trichrome staining of the tissue. Photomicrography of each slide was taken with a CKX41–32PHP inverted microscopic/digital camera (2002 Olympus Optical, Olympus, Tokyo, Japan). The images were digitally captured with an image scanner DP 70 controller system (Olympus, Japan) and were quantified by image analysis using Metamorph 6.0 software (Universal Imaging, Downingtown, PA, USA) according to the software manual. In brief, for each trichrome-stained liver section examined, five adjacent fields were captured at low-power magnification (five fields at low-power magnification were sufficient to cover the entire area of each liver section regardless of the location, such as periportal or perivenular), then we analyzed the total area (TA) of fibrosis (blue-stained area) and optical density (OD) of the five adjacent pictures. The degree of fibrosis of each liver section was defined as the mean total fibrotic area and OD of the five pictures of each liver section. This approach enabled us to measure the small area of fibrosis around the Disse space and central vein of each liver lobule.

Determination of the hepatic hydroxyproline content

Hepatic hydroxyproline content was measured colorimetrically in duplicates from 0.2 g liver tissue.[15] Briefly, the tissue was homogenized in 4 mL of 6 N HCl, then hydrolyzed at 110°C for 16 h. After filtering, 50 uL aliquots were evaporated, and residual HCl was removed after the addition of methanol. The sediment was dissolved in 50% isopropanol and incubated with 0.2 mL of 0.84% chloramine-T. Next, 1.0 mL of 12% Ehrlich's reagent was added and the mixture was incubated at 50°C for 90 min. The OD of the sample solution was measured at a 558 nm wavelength. The OD value was obtained by subtracting the OD of the reagent blank

from the OD of a sample. Hydroxyproline was quantitated from a standard curve with amino acid.

Immunohistochemistry for α-smooth muscle actin, transforming growth factor-β1, and COX-2

Immunohistochemical staining was performed on 5-μm tissue sections after deparaffinization in xylene and rehydration in a descending alcohol series. Antigen retrieval was performed by microwaving the tissue in a 0.01 mol/L citric saline buffer (pH 6.0). Endogenous peroxidase activity was quenched by H_2O_2 in phosphate-buffered saline (PBS) for 10 min. The sections were then washed in water and preblocked with normal goat or rabbit serum for 10 min. For the reaction with the primary antibody, the slides were incubated with monoclonal mouse anti-α-smooth muscle actin (α-SMA) antibody (Biomeda, Foster City, CA, USA, 1:20) or monoclonal mouse anti-transforming growth factor-β1 (TGF-β1) antibody (R&D system, 1:100) for 1 h. The sections were then incubated with biotinylated secondary antibodies (1:400) for 45 min. Following a PBS wash, the avidin–biotin complex (Strept ABComplex; DAKO, Carpinteria, CA, USA) was applied. Finally, the sections were rinsed in PBS, developed with diaminobenzidine tetrahydrochloride substrate for 3 min, and counterstained with hematoxylin. For the immunohistochemistry of the COX-2 expression, we used polyclonal rabbit antimurine COX-2 serum (Cayman Chemical, Ann Arbor, MI, USA) diluted to 2.5 μg/mL. Immunoreactive complexes were visualized with the peroxidase substrate 3-amino-9-ethyl-carbazole.

Sodium dodecyl sulfate–polyacrylamide gel electrophoresis and Western blot analysis

The frozen liver tissues were thawed at RT, weighed, placed in PBS (1:4 w/v), and homogenized with a Tissue-Tearor (Biospec, Bartlesville, OK, USA). The homogenate was sonicated three times for 20 s at RT and centrifuged at 12 000 rpm. for 10 min. The supernatant was diluted with electrophoretic sample buffer to obtain a total protein concentration of 39.2 μg/4 μL (9.8 μg/μL), then heated at 100 °C for 7 min. The heated samples were electrophoresed under denaturing conditions in a sodium dodecyl sulfate–polyacrylamide gel electrophoresis gel using a discontinuous procedure. The gels consisted of a 4.5% polyacrylamide stacking gel and 7.5% polyacrylamide separating gel. Paired mini-gels (Mini-protein II cell, Bio-Rad Laboratories, Hercules, CA, USA) were loaded with 39.2 μg protein/well. The protein concentration was estimated by the Bradford method. Samples containing the standard markers, including COX-2, matrix metalloproteinase (MMP)-9, and TGF-β, were run at 100 V/gel slab. After electrophoresis, one mini-gel was routinely stained with Coomassie blue and the other gel was equilibrated in transfer buffer (25 mM Tris, 192 mM glycine, and 20% methanol [v/v], pH 7.3). The proteins were then electrotransferred to a polyvinylpolypyrrolidone (PVDF) transfer membrane (Immunoblot TM PVDF membrane for the protein blot analysis, 0.2 μm; Bio-Rad, USA) at 50 V for 1 h at RT. To visualize the transferred proteins, the PVDF membrane was stained with Brilliant Blue R-250 (Sigma, St Louis, MO, USA) for 10 min and subsequently incubated in TBS (50 mM Tris/HCl and 20 mM NaCl, pH 7.4) containing 5% bovine serum albumin or TBS-T (TBS with 0.1% Tween-20) with 5% skim milk for 1 h at RT to block the non-specific sites. The blot was then rinsed with TBS-T. The COX-2 (antibody [Ab]-1), MMP-9 (Ab-1), TGF-β (Ab-1), and β-actin (Ab-1) proteins were detected by incubating the membrane in a moist chamber overnight at 4 °C with the following primary antibodies: rat anti-COX-2 (Ab-1, 1:200, Santa Cruz, Santa Cruz, CA, USA), rat anti-MMP-9 (Ab-1, 1:300, Biomeda, USA), rat anti-TGF-β (Ab-1, 1:200, R&D Systems), and rat anti-β-actin (Ab-1, 1:200, Santa Cruz, USA). After a TBS-T wash, the membrane was incubated with a secondary antibody (1:20,000, antimouse immunoglobulin G horseradish peroxidase-conjugate dilution, Biomeda, USA) for 2 h at RT. The peroxidase reaction was developed using an Amersham ECL reagent (Amersham Biosciences, Piscataway, NJ, USA). After imaging, the membranes were stripped and reprobed using a monoclonal anti β-actin antibody (Sigma, USA).

Enzyme-linked immunosorbent assay

First, the total protein was added to two 96-well polystyrene microplates (12 strips of eight wells) coated with a polyclonal antibody specific for mouse TGF-β. Second, for the capture antibody, we used a polyclonal antirat TGF-β antibody conjugated to horseradish peroxidase with preservatives. For the standard, we used 2.5 ng lyophilized recombinant rat TGF-β in a buffered protein base with preservatives. For the positive control, we used a lyophilized recombinant rat TGF-β protein in a buffered protein base with preservatives. The assay value of the control should be within the range specified on the control label. Third, we washed the plates with a wash buffer that consisted of a 25-fold concentrated solution of a buffered surfactant with preservatives. This buffer stabilized hydrogen peroxide and chromogen (tetram-

Table 1 Serum activities of AST, ALT, and the contents of Tbil determined after 3 weeks of experimental treatment

	AST (IU/L)	ALT (IU/L)	Tbil (mg/dL)
SO	76.95 ± 8.49	32.98 ± 5.23	0.16 ± 0.03
BDL	262.25 ± 74.25	96.26 ± 35.78	5.36 ± 2.01
BDL + Mel	193.25 ± 45.12*	70.07 ± 25.47*	4.13 ± 1.01*
Mel	84.53 ± 8.28	34.55 ± 4.67	0.19 ± 0.03

*$P < 0.05$ as compared with the bile duct ligation (BDL) group. Values are mean ± SD.
ALT, alanine transaminase; AST, aspartate transaminase; Mel, meloxicam; SO, sham operation; Tbil, total bilirubin.

ethylbenzidine). Finally, we added a diluted hydrochloric acid stop solution and determined the OD of each well within 30 min by measuring its absorbency at 450 nm using a microplate reader. If a wavelength correction was available, this correction was set to 540 or 570 nm. If wavelength correction was not available, the readings at 540 or 570 nm were subtracted from the readings at 450 nm. This subtraction was corrected for optical imperfections in the plate. Readings made directly at 450 nm without correction may be higher and less accurate. Immunoassays for COX-2 and MMP-9 were performed in a similar way (data not shown).

Statistical analysis

Statistical analysis was performed with SPSS software version 11.5 (SPSS, Chicago, IL, USA). Differences between two groups were analyzed by a Student's *t*-test. Differences between more than two groups were analyzed by ANOVA. *P*-values of less than 0.05 were considered statistically significant.

RESULTS

Effect of meloxicam on liver function test after 3 weeks of experimental treatment

BDL CAUSED AN increased concentration of the serum activities of AST, ALT, and the contents of Tbil. These were partially attenuated by treatment with meloxicam in the BDL rats (Table 1).

Three-week BDL induced ductular reaction and periportal fibrosis in rat livers

After 3-week BDL, the livers of the rats were grossly enlarged and lost their compliance when compared with the livers of the sham-operation rats (Fig. 1a). We found variable-sized, bile-filled, cell-lined biliary cysts that were proximal to the ligation site. Histologically, 3 weeks after the BDL, the livers showed portal-to-portal and portal-to-central linkage with fibrotic bands. Hepatocyte damage around the fibrous septa and fibrous streaks were significant in the rats that had undergone BDL for 3 weeks (Fig. 1d). We also noted that the rats with BDL had a minimal architectural distortion of their lobular structure, extensive bile duct proliferation that infiltrated into hepatocytes, and fibrogenesis in periportal area (Fig. 1d,e).

Meloxicam attenuated ductular reaction and collagen production in BDL-induced liver fibrosis

The livers of the group C rats were less edematous and had a better surface appearance when compared with group B (Fig. 1b). In the HE staining, meloxicam treatment suppressed both bile duct proliferation and periportal fibrogenesis (Fig. 1f). Masson's trichrome staining showed a clear-cut image of collagen deposition in the periportal blue-stained area. Meloxicam

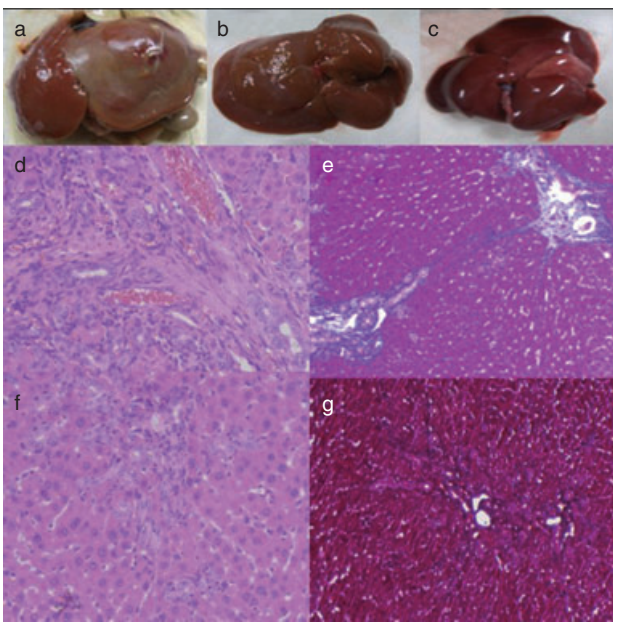

Figure 1 Representative findings of gross morphology (a–c), hematoxylin–eosin (d,f), and Masson's trichrome (e,g)-stained liver tissues obtained from rats after 3 weeks of experimental treatment (original magnification ×200). After bile duct ligation (BDL), we found a slight architectural distortion of the lobular structure, extensive bile duct proliferation infiltrating into the lobular hepatocytes, and occasional fibrogenesis in the parenchymal area (d,e). Meloxicam treatment in the BDL rats suppressed both bile duct proliferation and periductal fibrogenesis (f,g). (a,d,e) BDL; (b,f,g) BDL + drug; (c) drug.

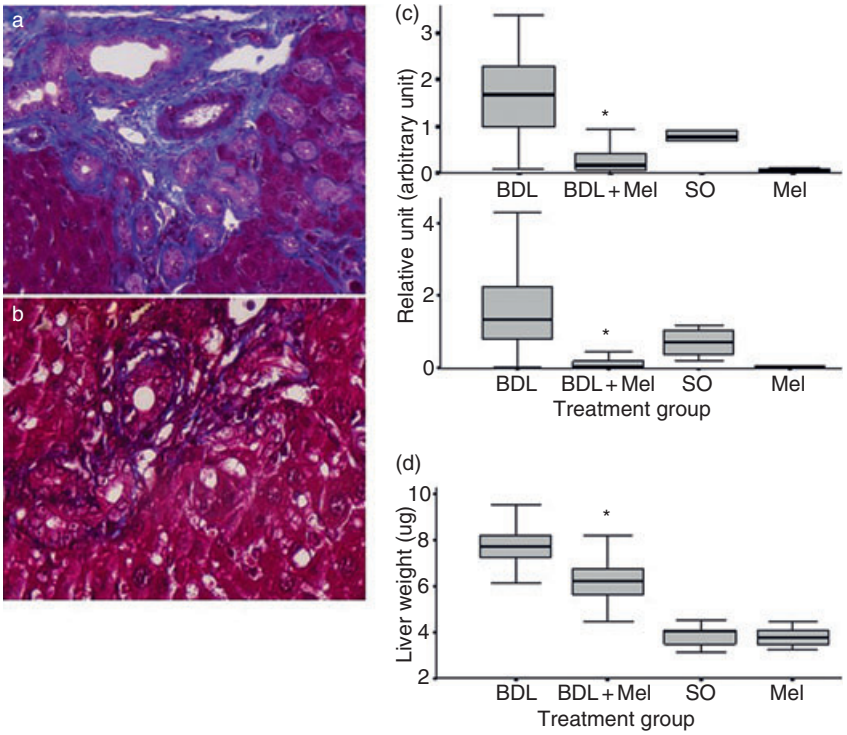

Figure 2 (a,b) Representative findings in Masson's trichrome-stained liver tissues obtained from rats after 3 weeks of experimental treatment (original magnification ×400). Periportal blue area indicates deposition of positively-stained collagen. Meloxicam (Mel) treatment in the bile duct ligation (BDL) rats attenuated bile duct proliferation and collagen production in myofibroblasts. (a) BDL; (b) BDL + drug. (c) Total area and optical density of the blue-stained collagen calculated by an image analyzer. Values were $5098.08 \pm 5200.96\ \mu m^2$ and 931.63 ± 629.76 degrees in group B and $567.68 \pm 1102.86\ \mu m^2$ and 173.6 ± 233.99 degrees in group C. (d) Quantification of the degree of liver fibrosis assessed by measuring hydroxyproline content in the liver. It was attenuated after Mel treatment. *Significantly different from BDL group ($P < 0.05$). SO, sham operation.

treatment in the BDL rats attenuated bile duct proliferation and periportal collagen deposition (Figs 1g,2b). The TA and OD of the blue-stained collagen areas were compared between groups B and C (Fig. 2c).

Meloxicam suppressed the expression of α-SMA, TGF-β, and COX-2 in livers of rats with BDL

At 3 weeks after BDL, α-SMA-expressing myofibroblasts were predominately located in the zone 1 areas and to a lesser degree in zones 2 and 3. Some of the α-SMA-expressing cells appeared to infiltrate into the lobular hepatocytes (Fig. 3a,b). Compared with group B, the group C rats had less bile duct proliferation and weak or no cytoplasmic α-SMA expression (Fig. 3c,d). A semi-quantitative analysis of α-SMA-positive cells showed that meloxicam reduced its number significantly (Fig. 3e). Immunohistochemical staining for TGF-β1 in the livers of BDL rats showed that the positively-stained, brown-colored cells were cholangiocytes in proliferating bile ductules and hepatocytes along the fibrous septa (Fig. 4a). Immunohistochemical staining for COX-2 showed that it was expressed in the proliferating bile ductules and to a lesser degree in the hepatocytes (Fig. 4B). Myofibroblasts around the periportal area showed weak or no staining for both TGF-β1 and COX-2. Compared with the group B rats, the livers of the group C rats showed reduced cytoplasmic TGF-β1 expression in the cholangiocytes and hepatocytes (Fig. 4c). Meloxicam treatment in the BDL rats also attenuated immunohistochemical staining for hepatic COX-2 in the cholangiocytes and hepatocytes (Fig. 4d).

Meloxicam suppressed profibrogenic cytokine TGF-β1, COX-2, and MMP-9 production in livers of rats with BDL

Enzyme-linked immunosorbent assay (ELISA) showed markedly reduced TGF-β1 production in the livers of group C rats when compared with group B ($P < 0.001$). A Western blot analysis of the TGF-β1 expression also showed similar results. Furthermore, the Western blot analysis and ELISA revealed that the hepatic production of COX-2 and MMP-9 proteins were reduced in group C rats as compared with group B (Fig. 5; Table 2).

DISCUSSION

IN THE PRESENT study, we determined that selective COX-2 inhibitor meloxicam suppressed liver fibrosis in a rat model of cholestatic liver disease. After 3 weeks

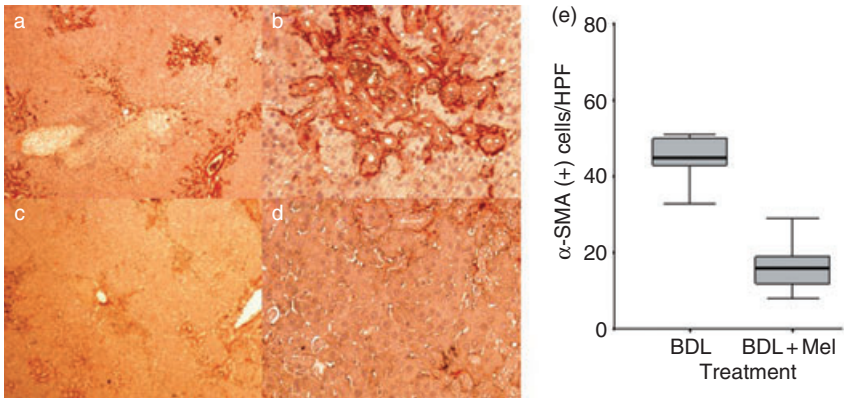

Figure 3 Representative findings of immunohistochemical staining for α-smooth muscle actin (α-SMA) in the livers of rats after 3 weeks of experimental treatment. In the bile duct ligation (BDL) rats, there were positively-stained portal myofibroblasts or activated hepatic stellate cells around the proliferating bile ducts in the periportal areas (a,b). Meloxicam (Mel) treatment in the BDL rats attenuated the positively-stained cells (c,d). For each specimen, the number of α-SMA-positive cells was counted in 10 high power fields (HPF) and expressed as the average number of α-SMA-positive cells/HPF (e). Mel significantly reduced the number of α-SMA-positive cells as compared with BDL ($P < 0.05$). (a,b) BDL, (c,d) BDL + drug. (Original magnification ×100 for a,c and ×200 for b,d.)

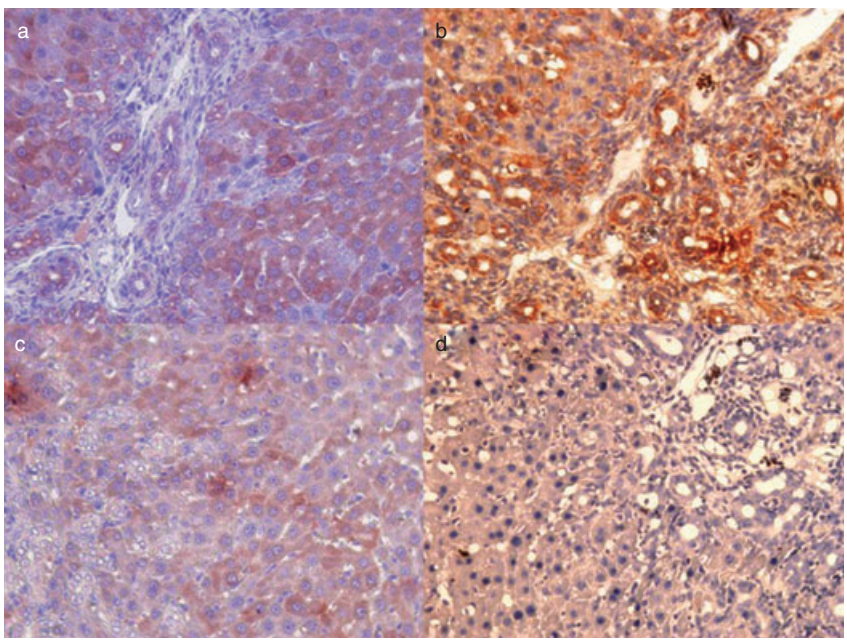

Figure 4 Immunohistochemical staining for transforming growth factor-β1 (TGF-β1) and cyclooxygenase-2 (COX-2) in livers of rats 3 weeks after bile duct ligation (BDL) (original magnification ×200). (a,c) Immunohistochemical staining of TGF-β1. At 3 weeks after BDL, positively-stained, brown-colored cells were mainly composed of proliferating bile ductules and hepatocytes along the fibrous septa. TGF-β1 staining was very faint in non-parenchymal cells in the fibrous septa (a). Meloxicam treatment in the BDL rats attenuated TGF-β1 staining in bile duct epithelial cells and hepatocytes (c). (b,d) Immunohistochemical staining of COX-2. At 3 weeks after BDL, the COX-2 expression was confined to cholangiocytes in proliferating bile ductules and hepatocytes and was not detected in non-parenchymal cells in the fibrous septa (b). Meloxicam treatment in the BDL rats attenuated COX-2 staining in bile duct epithelial cells and hepatocytes (d). (a,b) BDL; (c,d) BDL + drug.

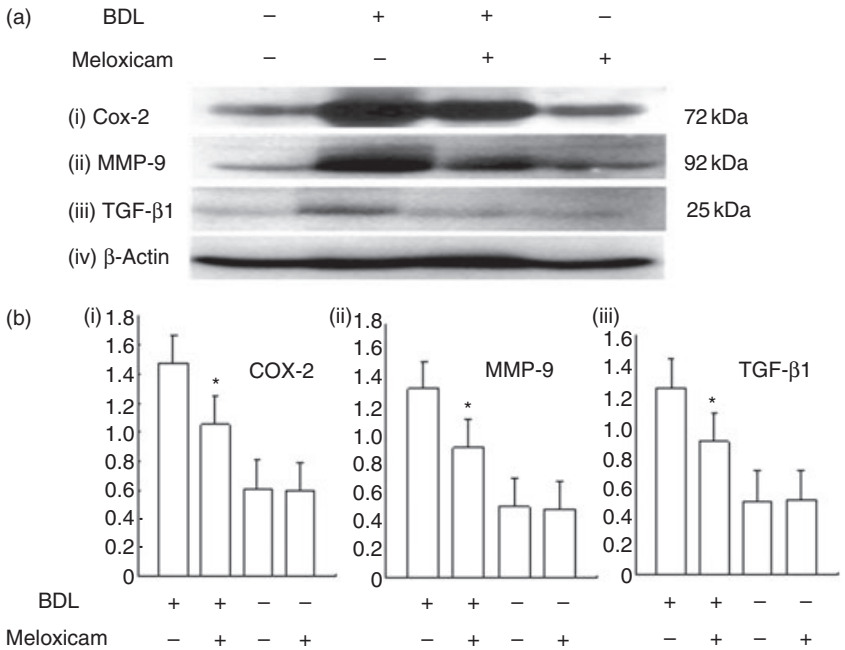

Figure 5 Total protein analysis of cyclooxygenase-2 (COX-2), matrix metalloproteinase-9 (MMP-9), and transforming growth factor-β1 (TGF-β1). (a) Western blot analysis shows that meloxicam suppresses the intensity of the bands of the COX-2 (72 kDa), MMP-9 (92 kDa), and TGF-β1 (25 kDa) proteins as compared with the bile duct ligation (BDL) rats. β-Actin served as a protein loading control. (i) COX-2 antibody (Ab): 1–2 ug/mL per total protein 200 ug/mL (ii) MMP-9 Ab: 1–2 ug/mL per total protein 300 ug/mL (iii) TGF-β1 Ab: 1–2 ug/mL per total protein 200 ug/mL (iv) β-actin Ab: 4.5 ug/mL per total protein 200 ug/mL (b) enzyme-linked immunosorbent assays also showed that meloxicam attenuated the expression of COX-2 (i), MMP-9 (ii), and TGF-β1 (iii) in the BDL rats. *Significantly different from BDL group ($P < 0.001$).

of BDL, we observed a marked proliferation of the cholangiocytes and portal fibroblasts around them. Proliferating bile duct epithelial cells in BDL showed increased COX-2 and TGF-β expressions when compared with neighboring hepatocytes and portal fibroblasts. All these changes were attenuated by meloxicam. Of major interest was the finding in the present work that in prolonged biliary obstruction, "reactive" biliary epithelia abandon their differentiated epithelial phenotype, and unlike normal cholangiocytes, have the ability to produce and secrete TGF-β1. This is in accordance with other previous reports.[16,17] There is increasing experimental evidence that bile acid (especially deoxycholic acid) promotes cholangiocyte proliferation by the activation of the epidermal growth factor receptor/mitogen-activated protein kinase/COX-2 signaling pathway.[18–20] Although it is uncertain from this study whether cholangiocyte proliferation is the result of the accumulated bile acid or BDL-induced hepatocyte damage, proliferating bile duct epithelial cells exclusively expressed COX-2. Therefore, it is highly likely that the COX-2 expression is critical in the activation and

Table 2 Enzyme-linked immunosorbent assay of COX-2, MMP-9, and TGF-β1 proteins after 3 weeks of experimental treatment

	COX-2	MMP-9	TGF-β1
SO	0.611 ± 0.077	0.502 ± 0.021	0.492 ± 0.044
BDL	1.478 ± 0.208	1.340 ± 0.270	1.244 ± 0.276
BDL + Mel	1.053 ± 0.245*	0.925 ± 0.192*	0.887 ± 0.135*
Mel	0.590 ± 0.054	0.489 ± 0.033	0.501 ± 0.044

*$P < 0.05$ as compared with bile duct ligation (BDL) group. Values are mean ± SD. COX-2, cyclooxygenase-2; Mel, meloxicam; MMP-9, matrix metalloproteinase-9; SO, sham operation; TGF-β1, transforming growth factor-β1.

proliferation of bile duct epithelial cells, which are able to secret TGF-β1. Recent studies have shown that selective COX-2 inhibitors can suppress nuclear COX-2 transcription as well as the biosynthesis of COX-2-dependent prostaglandins. Selective COX-2 inhibitors inhibit nuclear factor-κB activation through the inhibition of IκB (inhibitor of kappa B) kinase and Akt activation, leading to the downregulation of COX-2 synthesis and other genes needed for inflammation and proliferation.[21] In this respect, it is highly possible that meloxicam has the unique potential to suppress portal fibrosis in biliary obstruction. Reduced prostaglandin production by COX-2 inhibitors is a well-established concept of antifibrosis; that is, inflammation is the forerunner of fibrosis. Controlling the degree of inflammation can minimize the release of various inflammatory mediators known to be involved in collagen synthesis and accumulation, but in addition to that, we speculate from the current study that after BDL, the reactive biliary epithelia produce and secret profibrogenic TGF-β1 and that COX-2 is a critical intracellular signal pathway for this activation. Disruption of this signaling pathway may result in the loss of the regulation of cellular functions that govern the growth and survival of reactive cholangiocytes. Thus COX-2 inhibitors effectively ameliorate fibrosis in cholestatic injury. The major source of TGF-β1 in liver fibrosis has been considered to be damaged cells, such as hepatocytes or Kupffer cells, but the results of our experiment showed that TGF-β1 is expressed in almost all of the epithelial cells of the proliferating bile duct and some of the hepatocytes along fibrotic septa. This issue has not been the focus of much discussion, but is commensurate with a few previous studies about the cholestatic liver.[22–24] Ramm *et al*.[24] observed that CD68-positive macrophages within scar tissues did not contribute to TGF-β1 mRNA expression in biliary fibrosis. A few reports have shown that after BDL, TGF-β1 staining is well observed in hepatic stellate cells after BDL.[25,26] It is very difficult to explain based on the results of our study why TGF-β1 was expressed in peribiliary fibroblasts so weakly after BDL. Portal tract edema might cause tissue rarefaction in the peribiliary area, but we do not sure this really happened. We also speculate that this is related to the heterogeneity of the hepatic myofibroblast subpopulation (portal fibroblast *vs* sinusoidal hepatic stellate cell). In the current study, meloxicam also suppressed the TGF-β1 expression in the cholangiocytes and hepatocytes. It is uncertain from the present study whether COX-2 inhibitors directly affect TGF-β1 expression at the transcriptional level in the reactive cholangiocytes, but our finding is in line with other reports suggesting the inhibitory effect of selective COX-2 inhibitors on TGF-β1 expression.[27–29] In carbon tetrachloride-induced liver fibrosis, selective COX-2 inhibitors attenuate the expression of the connective tissue growth factor, which is a downstream effector of TGF-β.[11] Another *in vitro* study, however, showed that prostaglandin E_2 suppresses the expression of TGF-β1 and collagen α1(I) in hepatic stellate cells (HSC).[30] Further studies are needed to evaluate this important aspect (anti TGF-β1) of selective COX-2 inhibitors. In our study, TGF-β1-positive cells were still observed and their expression was higher than the sham-operation or drug-only group after treatment of meloxicam in the BDL group. Therefore, it is possible that COX-2 inhibitors might suppress hepatic fibrosis via another pathway. One of the candidates may be a peroxisome proliferator activated receptor-γ (PPAR-γ) pathway. PPAR-γ is a receptor transcription factor that controls growth and differentiation in various transformed cells such as HSC. It is widely accepted that selective COX-2 inhibitors are functional ligands of PPAR-γ for the inhibition of transdifferentiation of HSC.[10,31] With regard to the antifibrotic effect of the selective COX-2 inhibitors, one study has shown conflicting *in vivo* results that selective COX-2 inhibitor (celecoxib) aggravates CCl_4-induced rat liver fibrosis.[32] Ligation-induced biliary fibrosis seems to have quite different characteristics than toxin-induced fibrosis. The former is a consequence of proliferation of the bile duct epithelia and concentric proliferation of the portal fibroblasts around them. Lobular hepatocytes are preserved (zone 1 fibrosis). In contrast, CCl_4, applied intraperitoneally, is transported to the liver and is metabolized by hepatocytes. Subsequent cell death results in the production of cytokines like TGF-β1 and triggers the transdifferentiation process of perisinusoidal myofibroblast (HSC) in paracrine and autocrine loops (lobular fibrosis).[11,33] In biliary obstruction, portal fibroblasts rather than sinusoidal HSC are the major mesenchymal cells in the early stage.[34–36] In the present study, the expression of MMP-9 decreased after treatment of meloxicam. COX-2 promotes the release of MMP-2 and MMP-9 in rat fetal hepatocytes.[37] Their production is important for extracellular matrix remodeling that occurs in most liver fibrosis.[38] Meloxicam is a Food and Drug Administration-approved drug for rheumatoid arthritis and osteoarthritis.[39] It has become a recommended drug for use due to its preference for COX-2 over COX-1, lower gastrotoxicity, and lower cardiotoxicity than other selective COX-2 inhibitors.[14,40,41] In conclusion, the administration of COX-2 inhibitors leads to

a significant histological improvement, including the altered expression of several cytokines in BDL-induced liver fibrosis. The results of our study suggest that COX-2 inhibitors when used with ursodeoxycholic acid, may be beneficial in patients with progressive liver fibrosis, such as biliary atresia after portoenterostomy.

ACKNOWLEDGMENTS

THIS WORK WAS supported by a research grant from Yonsei University College of Medicine (6-2006-0044).

REFERENCES

1 Cheng J, Imanishi H, Iijima H *et al.* Expression of cyclooxygenase 2 and cytosolic phospholipase A(2) in the liver tissue of patients with chronic hepatitis and liver cirrhosis. *Hepatol Res* 2002; **23:** 185–95.
2 Mohammed NA, Abd El-Aleem SA, El-Hafiz HA, McMahon RF. Distribution of constitutive (COX-1) and inducible (COX-2) cyclooxygenase in postviral human liver cirrhosis: a possible role for COX-2 in the pathogenesis of liver cirrhosis. *J Clin Pathol* 2004; **57:** 350–4.
3 Yamamoto H, Kondo M, Nakamori S *et al.* JTE-522, a cyclooxygenase-2 inhibitor, is an effective chemopreventive agent against rat experimental liver fibrosis. *Gastroenterology* 2003; **125:** 556–71.
4 Dubois RN, Abramson SB, Crofford L *et al.* Cyclooxygenase in biology and disease. *FASEB J* 1998; **12:** 1063–73.
5 Zuo Y, Ma J, Gu Y, Yang H, Lin S. The renal protective effect of selective cyclooxygenase-2 inhibitor on obstructive nephropathy. *Zhonghua Nei Ke Za Zhi* 2002; **41:** 825–8.
6 Yao M, Lam EC, Kelly CR, Zhou W, Wolfe MM. Cyclooxygenase-2 selective inhibition with NS-398 suppresses proliferation and invasiveness and delays liver metastasis in colorectal cancer. *Br J Cancer* 2004; **90:** 712–19.
7 Nam KT, Hahm KB, Oh SY *et al.* The selective cyclooxygenase-2 inhibitor nimesulide prevents Helicobacter pylori-associated gastric cancer development in a mouse model. *Clin Cancer Res* 2004; **10:** 8105–13.
8 Chow LW, Loo WT, Toi M. Current directions for COX-2 inhibition in breast cancer. *Biomed Pharmacother* 2005; **59** (Suppl. 2)**:** S281–4.
9 Cheng J, Imanishi H, Liu W *et al.* Inhibition of the expression of alpha-smooth muscle actin in human hepatic stellate cell line, LI90, by a selective cyclooxygenase 2 inhibitor, NS-398. *Biochem Biophys Res Commun* 2002; **297:** 1128–34.
10 Planaguma A, Claria J, Miquel R *et al.* The selective cyclooxygenase-2 inhibitor SC-236 reduces liver fibrosis by mechanisms involving non-parenchymal cell apoptosis and PPARã activation. *FASEB J* 2005; **19:** 1120–2.
11 Tu CT, Guo JS, Wang M, Wang JY. Antifibrotic activity of rofecoxib *in vivo* is associated with reduced portal hypertension in rats with carbon tetrachloride-induced liver injury. *J Gastroenterol Hepatol* 2007; **22:** 877–84.
12 Aronson DC, Chamuleau RA, Frederiks WM, Gooszen HG, Heijmans HS, James J. Reversibility of cholestatic changes following experimental common bile duct obstruction: fact or fantasy? *J Hepatol* 1993; **18:** 85–95.
13 Hawk CT, Leary S. *Formulary for Laboratory Animals*. Ames, IA: Iowa State University Press, 1999.
14 Ogino K, Hatanaka K, Kawamura M, Katori M, Harada Y. Evaluation of pharmacological profile of meloxicam as an anti-inflammatory agent, with particular reference to its relative selectivity for cyclooxygenase-2 over cyclooxygenase-1. *Pharmacology* 1997; **55:** 44–53.
15 Jamall IS, Finelli VN, Que Hee SS. A simple method to determine nanogram levels of 4-hydroxyproline in biological tissues. *Anal Biochem* 1981; **112:** 70–5.
16 Lazaridis KN, Strazzabosco M, Larusso NF. The cholangiopathies: disorders of biliary epithelia. *Gastroenterology* 2004; **127:** 1565–77.
17 Gressner OA, Weiskirchen R, Gressner AM. Evolving concepts of liver fibrogenesis provide new diagnostic and therapeutic options. *Comp Hepatol* 2007; **6:** 7.
18 Werneburg NW, Yoon JH, Higuchi H, Gores GJ. Bile acids activate EGF receptor via a TGF-alpha-dependent mechanism in human cholangiocyte cell lines. *Am J Physiol Gastrointest Liver Physiol* 2003; **285:** G31–6.
19 Tsatsanis C, Androulidaki A, Venihaki M, Margioris AN. Signalling networks regulating cyclooxygenase-2. *Int J Biochem Cell Biol* 2006; **38:** 1654–61.
20 Yoon JH, Higuchi H, Werneburg NW, Kaufmann SH, Gores GJ. Bile acids induce cyclooxygenase-2 expression via the epidermal growth factor receptor in a human cholangiocarcinoma cell line. *Gastroenterology* 2002; **122:** 985–93.
21 Shishodia S, Koul D, Aggarwal BB. Cyclooxygenase (COX)-2 inhibitor celecoxib abrogates TNF-induced NF-κB activation through inhibition of activation of I kappa B alpha kinase and Akt in human non-small cell lung carcinoma: correlation with suppression of COX-2 synthesis. *J Immunol* 2004; **173:** 2011–22.
22 Saperstein LA, Jirtle RL, Farouk M, Thompson HJ, Chung KS, Meyers WC. Transforming growth factor-beta 1 and mannose 6-phosphate/insulin-like growth factor-II receptor expression during intrahepatic bile duct hyperplasia and biliary fibrosis in the rat. *Hepatology* 1994; **19:** 412–17.
23 Lee SY, Chuang JH, Huang CC *et al.* Identification of transforming growth factors actively transcribed during the progress of liver fibrosis in biliary atresia. *J Pediatr Surg* 2004; **39:** 702–8.
24 Ramm GA, Nair VG, Bridle KR, Shepherd RW, Crawford DH. Contribution of hepatic parenchymal and nonparenchymal cells to hepatic fibrogenesis in biliary atresia. *Am J Pathol* 1998; **153:** 527–35.

25 Xia JL, Dai C, Michalopoulos GK, Liu Y. Hepatocyte growth factor attenuates liver fibrosis induced by bile duct ligation. *Am J Pathol* 2006; **168:** 1500–12.
26 Osawa Y, Seki E, Adachi M *et al.* Systemic mediators induce fibrogenic effects in normal liver after partial bile duct ligation. *Liver Int* 2006; **26:** 1138–47.
27 Miyajima A, Ito K, Asano T, Seta K, Ueda A, Hayakawa M. Does cyclooxygenase-2 inhibitor prevent renal tissue damage in unilateral ureteral obstruction? *J Urol* 2001; **166:** 1124–9.
28 LaPointe MC, Mendez M, Leung A, Tao Z, Yang XP. Inhibition of cyclooxygenase-2 improves cardiac function after myocardial infarction in the mouse. *Am J Physiol Heart Circ Physiol* 2004; **286:** H1416–24.
29 Wang JL, Cheng HF, Shappell S, Harris RC. A selective cyclooxygenase-2 inhibitor decreases proteinuria and retards progressive renal injury in rats. *Kidney Int* 2000; **57:** 2334–42.
30 Hui AY, Dannenberg AJ, Sung JJ *et al.* Prostaglandin E2 inhibits transforming growth factor beta 1-mediated induction of collagen alpha1(I) in hepatic stellate cells. *J Hepatol* 2004; **41:** 251–8.
31 Lopez-Parra M, Claria J, Titos E *et al.* The selective cyclooxygenase-2 inhibitor celecoxib modulates the formation of vasoconstrictor eicosanoids and activates PPARã. Influence of albumin. *J Hepatol* 2005; **42:** 75–81.
32 Hui AY, Leung WK, Chan HL *et al.* Effect of celecoxib on experimental liver fibrosis in rat. *Liver Int* 2006; **26:** 125–36.
33 Lotersztajn S, Julien B, Teixeira-Clerc F, Grenard P, Mallat A. Hepatic fibrosis: molecular mechanisms and drug targets. *Annu Rev Pharmacol Toxicol* 2005; **45:** 605–28.
34 Clouzeau-Girard H, Guyot C, Combe C *et al.* Effects of bile acids on biliary epithelial cell proliferation and portal fibroblast activation using rat liver slices. *Lab Invest* 2006; **86:** 275–85.
35 Tuchweber B, Desmouliere A, Bochaton-Piallat ML, Rubbia-Brandt L, Gabbiani G. Proliferation and phenotypic modulation of portal fibroblasts in the early stages of cholestatic fibrosis in the rat. *Lab Invest* 1996; **74:** 265–78.
36 Beaussier M, Wendum D, Schiffer E *et al.* Prominent contribution of portal mesenchymal cells to liver fibrosis in ischemic and obstructive cholestatic injuries. *Lab Invest* 2007; **87:** 292–303.
37 Callejas NA, Casado M, Diaz-Guerra MJ, Bosca L, Martin-Sanz P. Expression of cyclooxygenase-2 promotes the release of matrix metalloproteinase-2 and –9 in fetal rat hepatocytes. *Hepatology* 2001; **33:** 860–7.
38 Guyot C, Lepreux S, Combe C *et al.* Hepatic fibrosis and cirrhosis: the (myo) fibroblastic cell subpopulations involved. *Int J Biochem Cell Biol* 2006; **38:** 135–51.
39 Ahmed M, Khanna D, Furst DE. Meloxicam in rheumatoid arthritis. *Expert Opin Drug Metab Toxicol* 2005; **1:** 739–51.
40 Martin RM, Biswas P, Mann RD. The incidence of adverse events and risk factors for upper gastrointestinal disorders associated with meloxicam use amongst 19,087 patients in general practice in England: cohort study. *Br J Clin Pharmacol* 2000; **50:** 35–42.
41 Ogino K, Saito K, Osugi T, Satoh H. Meloxicam (Mobic): a review of its pharmacological and clinical profile. *Nippon Yakurigaku Zasshi* 2002; **120:** 391–7.